

Effect of Ultrasonic Impact Treatment on the Structure and Properties of Al-Mg-Si Alloy

A.L. Berezina, T.O. Monastyrskaya*, G.I. Prokopenko, O.A. Molebny, S.S. Polishchuk, A.V. Kotko

Institute for Metal Physics of the NAS of Ukraine, 36 Vernadsky Blvd., 03680 Kyiv, Ukraine

((Received 07 June 2013; revised manuscript received 09 July 2013; published online 01 September 2013))

The study of the effect of ultrasonic impact treatment on the structure of Al-Mg-Si alloy surface showed that the initial structural state of the alloy significantly affected the mechanism of relaxation of internal stresses generated by shock-cyclic loading. The formation of orientation chaos observed in pre-homogenized alloy. Many nanoscale areas (20-50 nm wide and up to 80 nm long) of re-orientation matrix with random orientation formed on the surface of the specimen. After aging of the alloy to form a metastable β' phase, relaxation was due to the formation of non-crystallographic orientation bands with a high density of dislocations and ragged dislocation boundaries. It was found that the fragmentation of matrix or grain refinement was not observed during ultrasonic impact treatment of Al-Mg-Si alloy.

Keywords: Al-Mg-Si alloy, ultrasonic impact treatment, re-orientation band, orientation chaos.

PACS numbers: 68.35.bd, 68.37.Lp, 81.65.-b

1. INTRODUCTION

Numerous studies in recent years indicate that the severe plastic deformation (SPD) of metals and alloys leads to a significant increase in their mechanical properties and performances [1]. Surface SPD can significantly improve the mechanical properties such as fatigue strength and wear resistance, improve corrosion resistance [2]. An important task is to create a hardened surface with submicrocrystalline (grain size $d \sim 100 - 1000$ nm) and nanocrystalline ($d < 100$ nm) grain structure which has increased resistance to crack emergence and development. Several studies have shown the possibility of nanostructuring the surface of aluminum alloys using special modes SPD [3-6]. One of the methods of surface plastic deformation is ultrasonic impact treatment (UIT). During three-dimensional SPD the material is subjected to a static stress, and shock stress of the material occurs as a result of UIT. The use of high-power ultrasonic energy in the surface treatment of materials leads to fundamental changes in the structure of the surface and subsurface layers [7-10]. Micro- and nanostructures formed due to the use of UIT improve performances of materials. However, the structural mechanism of changes in the mechanical properties of thin surface layers produced using this technology has not been studied.

The formation of a submicrocrystalline and nanocrystalline structure in relatively inexpensive industrial aluminum alloys due to the use of SPD can transform low-strength alloys into medium-strength and high-strength ones. Aging aluminium alloys with nanostructures can be used for producing heavy-duty castings with high performances.

The possibility of changing the structure and properties of the wrought low-alloyed, low-cost Al-Mg-Si alloy of 6060 type by surface severe plastic deformation has been studied. The alloy has high plasticity, the ability for hot extrusion, and high corrosion resistance, which are excellent characteristics for various applications. The low strength of the alloy, however, is its main disadvantage. Of great interest is the search for

additional methods of hardening the alloy. The primary task of this research investigation has been to study the possibility of improving the mechanical properties of the alloy using surface severe plastic deformation in combination with different types of thermal treatments

2. EXPERIMENTAL

Wrought Al-Mg-Si alloy of 6060 type was chosen for investigation. Alloys of 6060 type are the basis of an important class of heat-hardenable wrought alloys. These alloys are inexpensive, and have a low alloying content of 1–2%, which is significantly less than that of widely used aluminum alloys of 2XXX type. The equilibrium phase diagram of the alloy is well studied. Quasibinary Al-Mg₂Si section is observed in the system when the ratio of Mg:Si is 1.73, where the compound Mg₂Si, or β -phase, located on the quasibinary section, is in equilibrium with the aluminium solid solution. Industrial wrought alloys contain 0.6-1.5% Mg₂Si, with a small excess of magnesium or silicon. Alloys are strengthened due to the precipitation hardening during the aging process as a result of the formation of metastable hardening β'' and β' phases, which have a coherent and a semicoherent relation with the matrix, respectively. The β' phase has a hexagonal lattice with parameters $a = 0.705$ nm, $c = 0.405$ nm, and precipitates in the form of needles and rods. The equilibrium β phase has a cubic *fcc* structure, with parameter $a = 0.635$ nm. The investigated Al-Mg-Si alloy is the one with the lowest volume fraction of Mg₂Si phase (0.6%) and, accordingly, exhibits the lowest hardening during aging of the 6XXX series alloys. The composition of the 6060 alloy is shown in Table 1.

Table 1 – The composition of aluminium alloys

Alloy	Concentration of elements (wt %)						
	Mg	Si	Fe	Cu	Ti	Mn	Zn
6060	0.59	0.50	0.31	0.06	0.032	0.037	0.06

A high-power ultrasonic energy was used for the surface treatment of materials. Cylindrical specimens of

* monast@imp.kiev.ua

the alloy with the diameter of 20 mm and the height of 0.8 mm were prepared. The ends of the samples were subjected to ultrasonic impact treatment at room temperature using UZG-300 installation. The specimens were placed in a special steel mandrel vibrating with the frequency of 15 Hz in the horizontal direction. Shock head with seven steel strikers, 5 mm in diameter, was placed on the edge of the hub of ultrasonic vibrations. Strikers produced forced vibrations between the hub of ultrasonic vibrations and the sample with the frequency of 2.1 kHz and caused shock hardening of its surface. The duration of treatment ranged from 25 to 50 s and the amplitude of ultrasonic vibrations was 23 μm .

The structure of the alloys in the initial state and after UIT was studied using transmission electron microscopy (JEM-2000FXII) and Vickers Hardness measurements. Phase composition of the alloy before and after UIT was determined by X-ray analysis (DRON-3M) using CoK α radiation. X-ray diffractometer DRON-UM1 was used to study the texture for specimens after UIT.

3. RESULTS AND DISCUSSION

3.1 Effect of UIT on the Structure and Properties of the Surface of the 6060 Alloy

Microhardness of specimens in the initial state and after the UIT is shown in Table 2.

Table 2 – Microhardness of the 6060 alloy

Treatment	H μ , MPa	
	initial state	after UIT
Homogenization at 560°C for 12 h	535	662
Homogenization + Quenching from 480°C + Aging at 185 °C for 6 h	678	745

3.2 Effect of UIT on the structure of the homogenized 6060 alloy

The conventional optic microscopy study showed that after homogenization the alloy had equiaxed grain structure with the grain size of 200-500 μm . The TEM study of the alloys structure was carried out. The rod-like coarse particles of the equilibrium β phase, ~200-600 nm long and ~50-60 nm thick, were present in the alloy in the homogenized state. The precipitation density of the particles was small; they were noncoherent with the matrix and associated with dislocations (Fig. 2a).

The surface structure. The TEM study showed that the main mechanism of relaxation of internal stresses on the surface of the specimen during the UIT was re-orientation of the matrix and formation of vacancies. A typical element of the substructure was dipole configuration of extinction contours, that characterized the formation of the re-orientation band, ~20-50 nm wide and up to 80 nm long (Fig. 2e). Also, high porosity of the matrix was observed. The pore size was 10-30 nm (Fig. 2f). Deformation-induced dissolution of the particles of the equilibrium β phase occurred. The re-orientation bands were zones of localized shift. The scheme of the band is shown in Fig.1

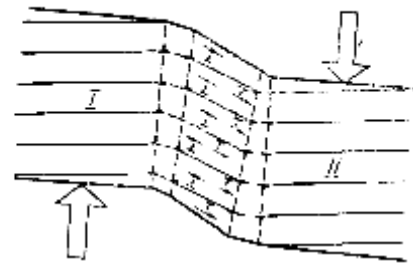


Fig. 1 – Scheme of the re-orientation band [11]

Noncrystallographic shift was carried out in the direction indicated by arrows due to the separation of dislocation charges, which was accompanied by a re-orientation of the lattice inside the band. The matrix orientation did not change. Re-orientation bands were located randomly (Fig. 2c) and formed substructure with a high curvature of the crystal lattice. These areas formed continuous diffuse electron diffraction rings, which indicated the formation of the orientation chaos (Fig. 2d).

The structure at ~70 μm distance from the surface.

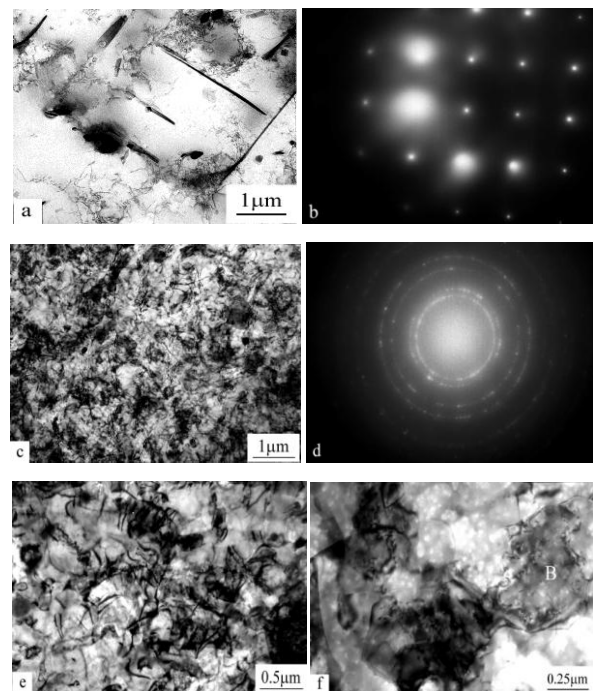


Fig. 2 – The structure (a) and electron diffraction (b) of the homogenized 6060 alloy; the structure (c) and electron diffraction (d) of the surface after the UIT; the extinction dipoles A (e); the porosity and re-orientation bands with ragged edges B (f)

The alloy structure was changed with increasing distance from the surface. Extinction dipoles disappeared and areas with the "speckled" contrast appeared. The areas were characterized by a high density of dislocation tangles. Net dislocation substructure was observed in some places. Border areas were ragged dislocation configurations. The appearance of such local metastable structures (zones of "flow") was believed to be the result of plastic strain relaxation in the case of high curvature of the lattice [12]. The appearance of "flow" zones did not lead to fragmentation and grain

refinement (Fig. 3a, b). However, electron-diffraction analysis (Fig. 3b) revealed that azimuthal diffuse tailing of matrix reflections was observed, which indicated the presence of internal stresses in the matrix. The cellular structure, as well as closed loop-like configurations of ragged dislocation boundary [13], was only found in a few places near β phase particles. Particles coagulation was observed in the matrix: shape factor of particles $k = l/h$ (ratio of length to width) was $\sim 20-60$ in the initial state and $k = 4 \div 6$ after the UIT.

3.3 Effect of UIT on the structure of the aged 6060 alloy

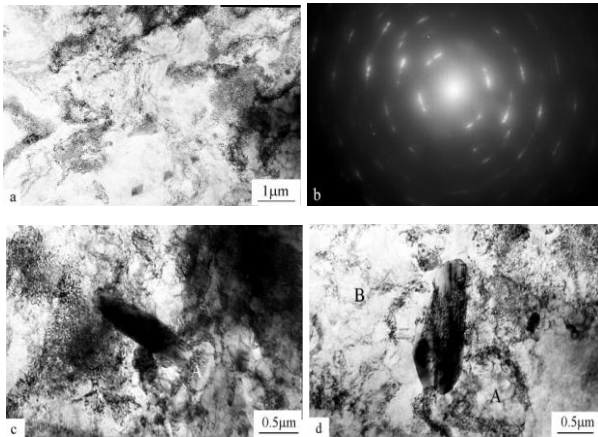


Fig. 3 – The inside of the homogenized 6060 alloy after UIT: the structure (a) and electron diffraction (b); interaction of the β phase particles with "flow" zones and the formation of loop-like configurations of ragged dislocation borders A (c) and cellular structure B (d).

Fine needle-like particles of the metastable β' phase (~ 20 nm long and $\sim 5-6$ nm thick) were formed in the matrix after the decomposition of the supersaturated solid solution (Fig. 4a). The particles had a high precipitation density, were coherently bound with the matrix and were strengthening precipitates.

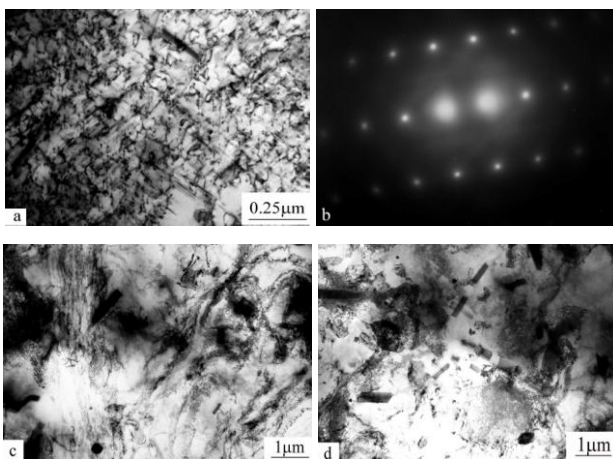


Fig. 4 – The structure (a) and electron diffraction (b) of the aged 6060 alloy; the surface of the aged alloy after UIT (c); the inside of the aged alloy after UIT (d).

An interaction of a shock wave with β' phase particles occurred during UIT of aged specimens. Metastable β' phase was replaced by a stable one, coalescence was

accelerated. Parallel areas of "flow" were observed as well as those which went around particles (Fig. 4 c, d). Grains refinement did not occur, but the internal stresses presented in the matrix because azimuthal diffuse tailing of matrix reflections in electron diffraction was observed.

3.4 X-ray Study

Phase analysis found a two-phase state: α -solid solution + stable Mg_2Si phase for specimen without UIT and for aged specimens after UIT (Fig.5). The phase composition of homogenized specimens after UIT changed - only reflexes of α -solid solution were present.

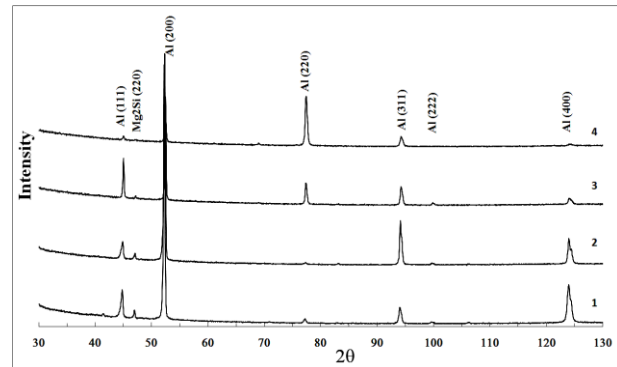


Fig. 5 – X-ray diffraction patterns of the 6060 alloy in the initial state: after homogenization at 560°C for 12 h (1), after quenching from 480°C and aging at 185°C for 6 h (2); after UIT: after quenching from 480°C and aging at 185°C for 6 h (3), after homogenization at 560°C for 12 h (4).

Comparison of profiles and intensities of the (400) reflexes from α -solid solution showed that after UIT Ka doublets were blurred and their intensities were significantly reduced, which could indicate both elastic distortions in the matrix and refinement of coherent scattering. Because refinement of the grain structure and block structure was not detected by TEM, it could be assumed that the decrease in the intensity of reflections was due to high internal stress in the matrix.

Anomalous ratio of the intensity of reflections from the matrix indicated the presence of texture. An increase in the intensity of the (220) reflexes after UIT indicated the emergence of a new texture component (Fig.5). The texture was studied for specimens after UIT. The ratio of texture component $\langle 100 \rangle$ and $\langle 111 \rangle$ is shown in Table 3.

Table 3 – Texture study of specimens after UIT

Specimens	Texture
Homogenization at 560°C for 12 h	65% $\langle 110 \rangle$ + 35% $\langle 100 \rangle$
Homogenization + Quenching from 480°C + Aging at 185°C for 6 h	85% $\langle 100 \rangle$ + 15% $\langle 111 \rangle$

4. CONCLUSIONS

1. Dependence of the relaxation mechanisms of internal stresses which were caused by shock cyclic loading during UIT and initial structural state of the Al-Mg-Si alloy was found.

2. Formation of many nanoscale re-orientation areas of the matrix with a random orientation was the main mechanism of stress relaxation on the surface of the specimen in the case of absence of the coherent metastable β' phase. Orientation chaos occurred.

3. The metastable β' phase, which was formed during aging, suppressed processes of matrix re-orientation. Relaxation was due to the formation of non-crystallographic orientation bands (elongated are-

as) with high density of dislocations and ragged dislocation boundaries.

4. UIT enabled the dissolution of excess phases, accelerated coalescence, replaced the metastable phase with the stable one.

5. Grain refinement was not observed during UIT of the Al-Mg-Si alloy. Strengthening was caused by internal stresses in the matrix. The increase in alloy microhardness after UIT was 24%.

REFERENCES

1. Ruslan Z. Valiev, Terence G. Langdon, *Progress in Materials Science* **51**, 881 (2006).
2. O. Sitdikov, T. Sakai, E. Avtokratova, R. Kaibyshev, Y. Kimura, K. Tsuzaki, *Materials Science and Engineering A* **444**, 18 (2007).
3. M. Sato, N. Tsuji, Y. Minamino et al., *Mater. Sci. Forum*, **426-432**, 2753 (2003).
4. X. Wu, N. Tao, Y. Hong et al., *Acta Mater.*, **50**, 2075 (2002).
5. A.S. Grinspan and R. Gnanamoorthy, *Appl. Surf. Sci.*, **253**, 989 (2006).
6. T. Ludian, L. Wagner, *Mater. Sci. Eng. A*, **468-470**, 310 (2007).
7. A.A. Kazimirov, A.A. Gruzd and G.I. Prokopenko, *Avt. Svarka*, №7, 38 (1980).
8. I.G. Polotskiy, G.I. Prokopenko, V.P. Krivko, *Metal Science and Heat Treatment*, №5, 46 (1983).
9. B.N. Mordyuk and G.I. Prokopenko, *J. Sound Vibration*, **308**, 855 (2007).
10. M. Liao, W.R. Chen and N.C. Bellinger, *Inter J. Fatigue*, **30**, 717 (2008).
11. A.D. Korotaev, A.N. Tjumentsev, V.F. Suhovarov, *Dispersion hardening of refractory metals* (Novosibirsk: Science, Siberian Branch: 1989).
12. *Structural levels of plastic deformation and fracture*, (Ed. V.E. Panin) (Novosibirsk: Science, Siberian Branch: 1990).
13. V.V. Rybin, *Large plastic deformations and fracture of metals*, (Moscow: Metallurgy: 1986).